The impacts of image resolution on permeability simulation of gas diffusion layer using lattice Boltzmann method

THE IMPACTS OF IMAGE RESOLUTION ON PERMEABILITY SIMULATION OF GAS DIFFUSION LAYER USING LATTICE BOLTZMANN METHOD

Jinuntuya, F.[1], Chen, R.[1], Ostadi, H.[2], Jiang, K.[2], Gao, Y.[3], Zhang, X.[3]

[1]Department of Aeronautical and Automotive Engineering, Loughborough University, Leicestershire LE11 3TU, UK
[2]Centre for Biomedical and Nanotechnology, School of Mechanical Engineering, University of Birmingham, Birmingham B15 2TT, UK
[3]Department of Engineering, University of Liverpool, Liverpool L69 3GH, UK

Corresponding author: Fontip Jinuntuya (F.Jinuntuya@lboro.ac.uk)

The effect of image resolution on gas permeability through the x-ray reconstructed carbon paper gas diffusion layer (GDL) of a polymer electrolyte fuel cell (PEFC) is examined in this paper. The 3D models of the GDL at six different resolutions are obtained by the x-ray tomography imaging technique. Each GDL image is then characterized its gas permeability through the lattice Boltzmann (LB) numerical method. The results suggest that the image resolution has a great impact on gas permeability in both principal and off-principal flow directions. The coarser resolutions can contribute to significant changes in the resulting permeability. However, it can reduce computational time to a great extent. The results also indicate that the GDL image at the resolution of 2.72 μm provides a good compromise between computational time and accuracy.

Keywords: Gas diffusion layer, lattice Boltzmann method, x-ray tomography

Introduction

Gas diffusion layer plays an important role in the overall performance and durability of a PEFC by serving several functions including providing pathways for reactant gases to access the reaction sites; product water removal; heat and electronic transport and also serving as a mechanical support for the membrane. The GDL is a heterogeneous porous carbon-based material typically made of woven carbon cloth or non-woven carbon paper with a thickness in the order of 100 μm [1]. To date, experimental measurements of fluid flows and related parameters in such a complicatedly diminutive size of the GDL remain difficult. Therefore, several pore-scale numerical models have been extensively developed and applied to examine fluid transport through the GDL.

Among various approaches, the LB method has been increasingly utilized to investigate fluid transport in a porous geometry like the GDL. This is because it has the capability to implement boundary conditions in such complex porous structures by imposing the bounce-back scheme where it is assumed that any particle that hit the solid boundaries simply bounce-back to its original position [2]. With such treatment, the LB method is technically superior to the well-established conventional CFD method where the incorporation of boundary-fitted grid in a complicated boundary is extremely difficult.

Recently, in order to accurately reflect the actual GDL as manufactured, the x-ray computed tomography reconstruction technique has been employed to generate 3D representative structures of GDL samples. The combination of the two advanced techniques has also been successfully applied to study fluid movement through PEFC GDLs in recent publications [2-

8]. However, the computational demanding of the LB method together with a tendency to use the highest available resolution of the x-ray imaging facility has limited its application to analyze only a very small volume of the GDL. With such high resolutions, the LB flow simulation is also extremely time-consuming.

In this work, the effect of image resolution on gas permeability through the x-ray reconstructed GDL was examined by using the LB method. The binary 3D models of the GDL at 6 different resolutions were acquired by using the x-ray imaging technique. Each image was then integrated into a single-phase LB numerical solver to characterize its gas permeability. The resulting permeability, its sensitivity to the resolution variation and the computational time were analyzed to identify the optimum resolution for the representative model of the GDL.

Methodology, Results and Discussion

Lattice Boltzmann method

In this study, the single-phase LB model is used to simulate gas flow through the GDL. Principally, the LB method tracks the movement and collisions of a number of fictitious fluid particles in a lattice domain. The movement of each fictitious particle is described by the particle distribution function $f_i(x,t)$ which defines the mass of a particle at location x and time t moving with the velocity ξ_i along the direction i [2]

$$f_i\left(x+\xi_i\delta t, t+\delta t\right) = f_i\left(x,t\right) + \frac{1}{\tau}\left[f_i^{eq}\left(x,t\right) - f_i\left(x,t\right)\right] \tag{1}$$

where $f_i^{eq}(x,t)$ is the value of $f_i(x,t)$ at an equilibrium state and τ is the dimensionless relaxation parameter that control the rate at which $f_i(x,t)$ approaches $f_i^{eq}(x,t)$. For incompressible flow, the $f_i^{eq}(x,t)$ is calculated from

$$f_i^{eq}\left(x,t\right) = w_i\left\{\rho + \rho_0\left[\frac{\xi_i\cdot u}{c_s^2} + \frac{1}{2}\left(\frac{\xi_i\cdot u}{c_s^2}\right)^2 - \frac{u\cdot u}{2c_s^2}\right]\right\} \tag{2}$$

where w_i is a weighting factor depending on the magnitude of the velocity ξ_i, c_s is the speed of sound. The fluid density ρ and fluid velocity u are calculated by summing the corresponding moments of all incoming particles at each node in the lattice domain as follows

$$\rho = \sum_i f_i = \sum_i f_i^{eq} \tag{3}$$

$$\rho_0 u = \sum_i f_i\xi_i = \sum_i f_i^{eq}\xi_i \tag{4}$$

The D3Q19 LB scheme is employed in this work where fluid particles in each lattice node are able to move in 19 directions from the origin in the 3-dimensional regime as shown in Fig. 1.

The LB implementation involves a collision step and a streaming step. In a collision step, the right-hand side of eq. (1) is calculated as $f_i^*(x,t) = f_i(x,t) + \left[f_i^{eq}(\rho,u) - f_i(x,t)\right]/\tau$. The streaming step moves the outcomes of collisions $f_i^*(x,t)$ from the location x to the nearest location $x+\delta t\xi_i$ along their direction of motion at time $t+\delta t$ to become $f_i\left(x+\delta t\xi_i, t+\delta t\right) = f_i^*\left(x,t\right)$. After the streaming step has been completed, the gas density ρ

and velocity u for each node in the lattice domain are updated through $\rho\left(x,t+\delta t\right)=\sum_i f\left(x,t+\delta t\right)$ and $\rho_0 u=\sum_i f_i\left(x,t+\delta t\right)$, respectively [2].

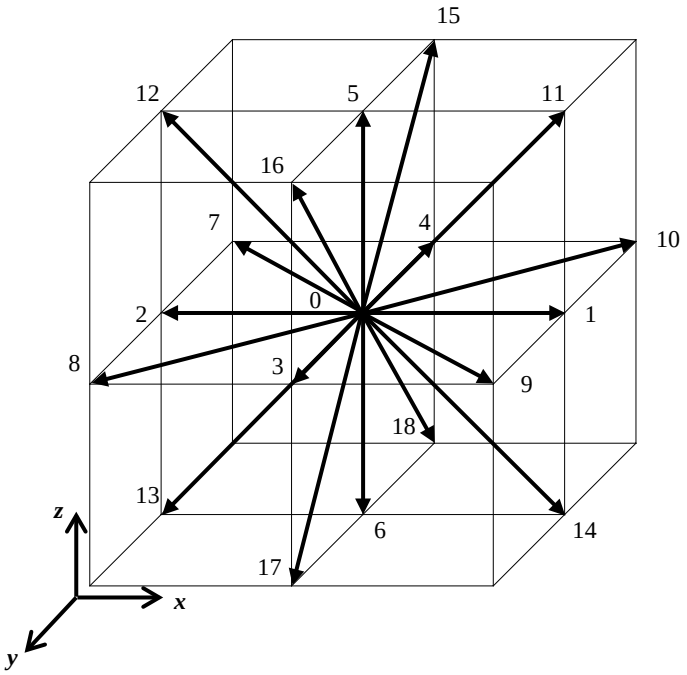

Fig. 1 The nineteen velocity directions in the D3Q19 LB scheme.

Permeability calculation

In this work, the permeability of the GDL is calculated from the detailed gas velocity distribution across the domain at the microscopic scale which is obtained by the LB simulation. The absolute permeability of the GDL at macroscopic scale is defined by Darcy's law as

$$k=\frac{\rho\mu q}{\left(\Delta P/L\right)} \tag{5}$$

where ρ is the gas density, q is the average gas velocity through the GDL in the direction of the pressure gradient, ΔP is the applied pressure gradient across the GDL image, L is the size of the domain and μ is the dynamic viscosity. The dynamic viscosity is related to the dimensionless relaxation time as follows

$$\mu=\delta x^2\left(\tau-0.5\right)/3\delta t \tag{6}$$

By applying a pressure gradient in the through-plane direction, gas can also flow in the in-plane direction. The three components of permeability tensor in principal and off-principal flow directions can be calculated as

$$k_{zz}=\frac{\rho\mu q_z}{\left(\Delta P/L_z\right)} \tag{7a}$$

$$k_{yz}=\frac{\rho\mu q_y}{\left(\Delta P/L_y\right)} \tag{7b}$$

$$k_{xz}=\frac{\rho\mu q_x}{\left(\Delta P/L_x\right)} \tag{7c}$$

where q_x, q_y, q_z are the average velocities and L_x, L_y, L_z are the sizes of the domain in x, y, z directions, respectively. The average velocities in the three directions are

$$q_x = \frac{\sum_i u_x(x_i)}{L_x L_y L_z} \tag{8a}$$

$$q_y = \frac{\sum_i u_y(x_i)}{L_x L_y L_z} \tag{8b}$$

$$q_z = \frac{\sum_i u_z(x_i)}{L_x L_y L_z} \tag{8c}$$

Digital 3D model

In this study, the digital image of a carbon paper GDL sample was originally generated at the resolution of 0.68 μm/pixel through the x-ray tomography imaging technique. In general, there are three key steps to generate the 3D images including progressive 2D imaging via x-ray tomography, image processing, and digital 3D reconstruction. The details of the x-ray tomography and digital reconstruction of the GDL were reported in [2, 3].

In order to examine the pixel size effect on the absolute permeability, a number of 3D images were then further generated based on the original resolution starting with 2 times up to 6 times larger than the original pixel size. Therefore, the GDL images with the resolution of 0.68, 1.36, 2.04, 2.72, 3.40, and 4.08 μm/pixel, repectively were employed to study the impact on the resulting permeability.

Fig. 2 shows the microstructure of the GDL sample with the size of 211 μm × 204 μm × 224 μm. The overall reconstructed GDL images of all 6 resolutions are then divided into 4 regions equally as shown in Fig. 3 while Fig. 4 illustrates the images of the 6 different resolutions of the region 1 which are used in this study. The size of each region in voxels and physical dimensions for each resolution are shown in Table 1.

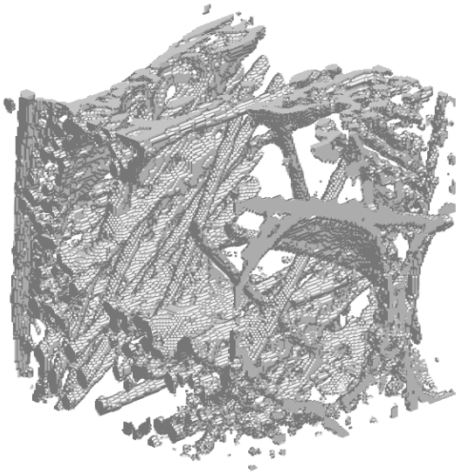

Fig. 2 Digital 3D image of the GDL sample.

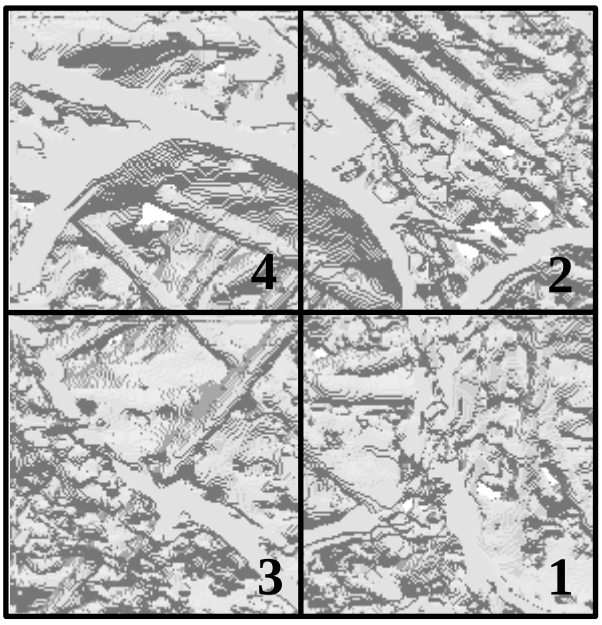

Fig. 3 GDL image with 4 regions of interest.

Table 1 Digital and physical image size of each region of the 3D GDL image with 6 different resolutions.

Resolutions (μm/pixel)	**Image size in voxels**			**Image size in μm**		
	x	**y**	**z**	**x**	**y**	**z**
0.68	155	150	329	105.40	102.00	223.72
1.36	78	75	164	106.08	102.00	223.04
2.04	52	50	109	106.08	102.00	222.36
2.72	39	38	82	106.08	103.36	223.04
3.40	31	30	65	105.40	102.00	221.00
4.08	26	25	54	106.08	102.00	220.32

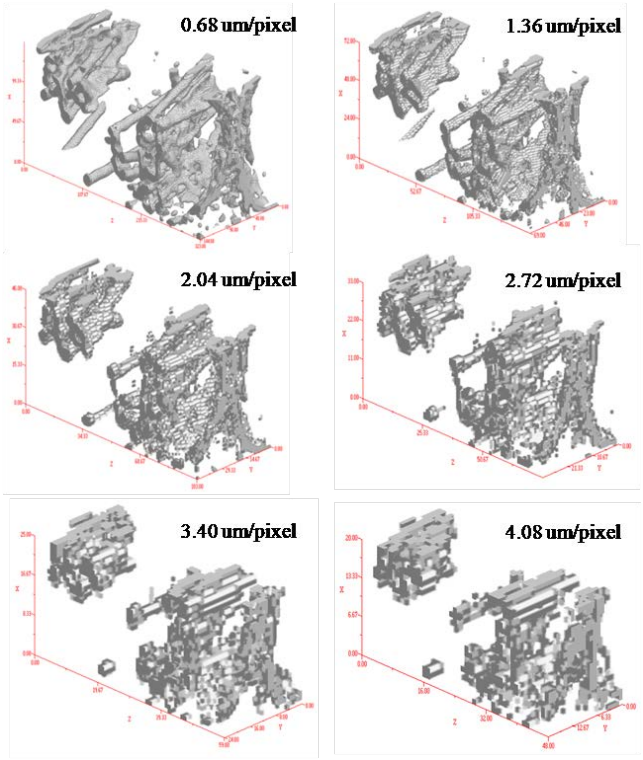

Fig. 4 Binary images of region 1 with 6 different resolutions including 0.68, 1.36, 2.04, 2.72, 3.40 and 4.08 μm/pixel, respectively.

Simulated permeability

The single-phase LB model was applied to each of the 4 regions of the GDL images reconstructed with the 6 different resolutions including 0.68, 1.36, 2.04, 2.72, 3.40 and 4.08 μm/pixel. To simulate the gas flow through the GDL, the pressure difference of 10 Pa is applied to each region and the void spaces are assumed to be filled with air. The principal flow direction is set in the through-plane direction along the GDL thickness. The detailed gas velocity field obtained from the LB simulation is then used to predict the gas permeability through the simulated GDL domain by using Darcy's law. All simulations are carried out on a quad-core 2.33 GHz workstation with 3.25 GB RAM.

Fig. 5(a)-(c) illustrate the simulated permeability when the pressure gradient is imposed in the principal through-plane flow direction (z-direction) and the simultaneous permeability in the off-principal in-plane flow directions (y- and x- directions). According to Fig. 5(a)-(c), the gas permeability in all flow directions varies locally among each simulated region thus the means are properly considered as the representative values for all regions. The mean simulated values of the gas permeability both in principal through-plane and off-principal in-plane flow directions, the mean porosity and the average calculation time for each of 6 resolutions are given in Table 2.

Table 2 Average porosity, through-plane, in-plane permeability in y- and x- direction and calculation time in each region of 6 different resolutions.

Resolutions (μm/pixel)	**Ave. porosity (%)**	**Ave. through-plane permeability**	**Ave. in-plane permeability y-direction**	**Ave. in-plane permeability x-direction**	**Ave. calculation time**

		(mm^2)	(mm^2)	(mm^2)	(min)
0.68	89.57	15.7332	1.2022	1.0981	1620
1.36	88.61	14.6168	1.3642	1.1893	63
2.04	87.15	12.5515	1.2353	1.1845	10
2.72	87.52	14.3591	1.2612	1.1006	4
3.40	87.60	17.2916	1.5874	1.2636	1
4.08	87.40	20.2754	1.4397	1.3783	<1

The results indicate that the variation of the image resolution contributes to a great difference on the predicting permeability in all flow directions. Assuming that the GDL image reconstructed by the original resolution of 0.68 μm provides the most accurate set of permeability values, all sets of results show that the differences are up to 30%, 32% and 26% for the resulting through-plane and in-plane permeability in y- and x- directions, respectively over the range of resolutions. The lowest resolution of 4.08 μm gives a huge change in the resulting permeability as expected, but on the other hand, it leads to a massive reduction in terms of computational time from approximately 1620 minutes per each region of the original resolution to just less than 1 minute.

The results also indicate that the GDL image at the resolution of 2.72 μm provides a good compromise between accuracy and simulation time. The resulting permeability values are less than 8%, 5% and 0.3% difference for the through-plane, in-plane permeability in y- and x- direction, respectively while the calculation time reduces greatly to just 4 minutes which is approximately 400 times less than the original resolution. By utilizing the 2.72 μm resolution, simulations are also able to analyze the gas flow characteristics in a 64 times larger in terms of domain size.

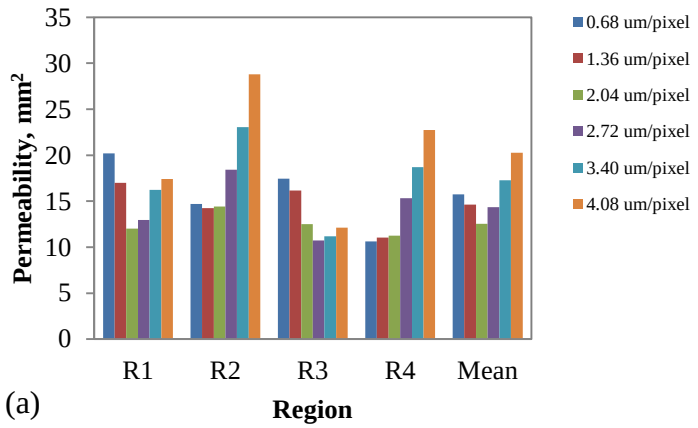

(a)

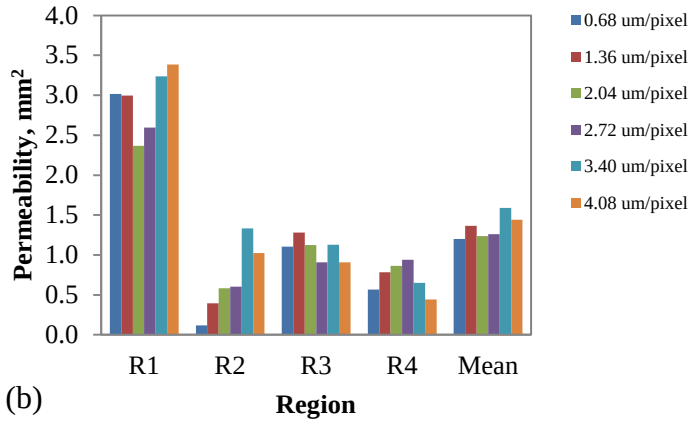

(b)

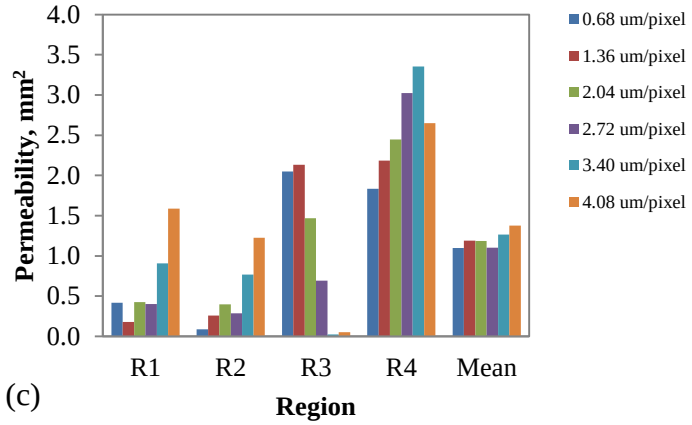

(c)

Fig. 5 Simulated absolute permeability in (a) through-plane direction (z-direction); (b) in-plane y-direction; (c) in-plane x- direction; for the 4 regions with 6 different resolutions including the mean values.

Conclusions

This study was conducted using the LB method and the x-ray computed tomography technique. The 3D models of the GDL at 6 different resolutions were generated via the x-ray reconstruction technique. Each of the images was then incorporated into the LB solver to predict its permeability. The effect of image resolution on gas permeability through the representative models of the actual GDL was studied. It was found that the resolution variation has a great impact on the resulting permeability in both principal and off-principal flow directions. The coarser resolutions contribute to significant changes in resulting average permeability up to 30% and 32% for the principal and off-principal flow directions, respectively. Conversely, the average calculation time reduces greatly from 27 hours to less than 1 minute over the range of resolutions. The results also suggest that the GDL image at the resolution of 2.72 μm, a 4 times larger than the original resolution, gives a good compromise for permeability simulation. In addition, with this resolution it is possible to investigate gas flows in a 64 times larger domain.

In conclusion, it is worth considering the effect of image resolution to identify an optimum resolution for the representative GDL model which potentially improve computational efficiency in terms of simulation time reduction then substantially lowering computational

costs or even allow simulation in a greater GDL volume while the accuracy is still satisfactory.

References

1. Mathias, M., Roth, J., Fleming, J. & Lehnert, W. (2003). *Handbook of Fuel Cells – Fundamentals, Technology and Applications, Vol. 3: Fuel Cell Technology and Application*, Wiley, New York, p. 517–538.
2. Rama, P., Liu, Y., Chen, R., Ostadi, H., Jiang, K., Zhang, X., Fisher, R., & Jeschke, M. (2010). An X-Ray Tomography Based Lattice Boltzmann Simulation Study on Gas Diffusion Layers of Polymer Electrolyte Fuel Cells. *Journal of Fuel Cell Science and Technology*, **7(3)**, p. 031015.1-031015.12.
3. Ostadi, H., Rama, P., Liu, Y., Chen, R., Zhang, X., & Jiang, K. (2010). Nanotomography based study of gas diffusion layers. *Microelectronic Engineering*, **87(5-8)**, p. 1640-1642. doi:10.1016/j.mee.2009.10.027
4. Rama, P., Liu, Y., Chen, R., Ostadi, H., Jiang, K., Zhang, X., Gao, Y., Grassini, P., & Brivio, D. (2010). Determination of the anisotropic permeability of a carbon cloth gas diffusion layer through X-ray computer micro-tomography and single-phase lattice Boltzmann simulation. *International Journal for Numerical Methods in Fluids*, **67(4)**, p. 518-530.
5. Rama, P., Liu, Y., Chen, R., Ostadi, H., Jiang, K., Zhang, X., Gao, Y., Brivio, D., & Grassini, P. (2011). A Numerical Study of Structural Change and Anisotropic Permeability in Compressed Carbon Cloth Polymer Electrolyte Fuel Cell Gas Diffusion Layers. *Fuel Cells*, **11(2)**, p. 274-285.
6. Ostadi, H., Rama, P., Liu, Y., Chen, R., Zhang, X. X., & Jiang, K. (2010). 3D reconstruction of a gas diffusion layer and a microporous layer. *Journal of Membrane Science*, **351(1-2)**, p. 69-74. doi:10.1016/j.memsci.2010.01.031
7. Ostadi, H., Rama, P., Liu, Y., Chen, R., Zhang, X. X., & Jiang, K. (2010). Influence of threshold variation on determining the properties of a polymer electrolyte fuel cell gas diffusion layer in X-ray nano-tomography. *Chemical Engineering Science*, **65(6)**, p. 2213-2217. Elsevier. doi:10.1016/j.ces.2009.12.019
8. Gao, Y., Zhang, X., Rama, P., Liu, Y., Chen, R., Ostadi, H., & Jiang, K. (2012). Calculating the Anisotropic Permeability of Porous Media Using the Lattice Boltzmann Method and X-ray Computed Tomography. *Transport in Porous Media*, **92(2)**, p. 457-472. doi: 10.1007/s11242-011-9914-7